find $Q_x = -7.6 \times 10^{-10}$ hartree, $Q_y = -2.0 \times 10^{-9}$ hartree, and $Q_z = 2.7 \times 10^{-9}$ hartree. Then $eq_x = -0.44$ au, $eq_y = -1.1$ au, and $eq_z = 1.6$ au. For $^{63}Cu$, $Q_x = -7.1 \times 10^{-10}$ hartree, $Q_y = -2.2 \times 10^{-9}$ hartree, $Q_z = 2.9 \times 10^{-9}$ hartree, $eq_x = -0.38$ au, $eq_y = -1.2$ au, and $eq_z = 1.6$ au.

This compound has nuclear quadrupole coupling constants consistent with the few other $^{63}Cu(II)$ oxygen-coordinated compounds of this high symmetry, mostly octahedral, that have been examined (ref 1-5, 8-10, and 14 and Table III). This system is a slightly elongated octahedron. Its QD value is at the low end of the range of values previously found for octahedral environments but above values found for more elongated octahedra.[14] The inclusion of the QE parameter here could account for the observed reduction in the QD value. The large QD (or $eq_z$) value indicates an elongated distribution of charge, mainly attributable to the $d_{xy}$ orbital vacancy in the Cu(II) valence shell, with some reduction—perhaps 25%—owing to covalent charge spreading.[4-6,10,12,23] Quantitative discussions of the relationship between QD, QE, and electronic structure are given elsewhere (e.g., ref 5, 9, 10, and 23, and work to be published). The QE value indicates some distortion from a completely axial charge distribution. The moderate rhombic component of that distribution ($eq_x - eq_y = 0.8$ au) must be related to a slight difference between two pairs of equatorial metal-oxygen bond distances revealed by the structural report on the host crystal.[19]

Finally, the utility of EPR powder spectra to determine nuclear quadrupole coupling constants has been confirmed in this study. Our predictions as well as the values initially derived from computer simulations of powder spectra were borne out by the subsequent detailed single-crystal analyses. The close agreement between the sets of EPR parameters obtained by the two methods demonstrates the adequacy of powder-spectrum simulation for the determination of nuclear quadrupole coupling constants.

**Acknowledgment.** This research was supported by the National Science Foundation, Quantum Chemistry Program.

**Registry No.** $MgSO_4 \cdot 7H_2O$, 25102-34-5; $^{63}Cu$, 14191-84-5; $^{65}Cu$, 14119-06-3.

(23) White, L. K. Ph.D. Thesis, University of Illinois, Urbana, IL, 1975.

Contribution from the Department of Chemistry, University of Iowa, Iowa City, Iowa 52242

# Multinuclear Magnetic Resonance Spectroscopy of Spin-Admixed $S = {}^5/_2, {}^3/_2$ Iron(III) Porphyrins

ARDEN D. BOERSMA and HAROLD M. GOFF*

*Received March 16, 1981*

A variety of synthetic iron(III) porphyrin complexes ($Fe^{III}PorX$, X = $SO_3CF_3^-$, $ClO_4^-$, and $C(CN)_3^-$) were examined with multinuclear NMR spectroscopy ($^1H$, $^{13}C$, $^{19}F$, and $^{35}Cl$). Deviations from NMR Curie law behavior, diminished magnetic moments, and characteristic ESR $g = 4$ values support previous evidence for the quantum-mechanical admixture of $S = {}^5/_2$ and $S = {}^3/_2$ states. NMR studies of titrations with the corresponding tetrabutylammonium salts and dipolar shift calculations show the ligands are coordinated rather than ion paired in solution. Solvent studies indicate more $S = {}^5/_2$ character is present in aromatic solvents than in chlorinated solvents. Although the tricyanomethanide complex is thought to exhibit a "pure" $S = {}^3/_2$ state in crystalline form, solution measurements are consistent with spin admixture.

## Introduction

Fundamental inorganic chemical studies have demonstrated that metalloporphyrins may exhibit fascinating and often unique structural, electronic, and reactivity properties. This is illustrated, for example, in the possible spin states of iron(III) porphyrins. The high-spin state is associated with coordination of a single weak-field anionic ligand or bisligation of two weak-field ligands.[1-3] Recently an unusual spin-admixed state of $S = {}^5/_2$ and $S = {}^3/_2$ character has been postulated for certain very weak-field anionic complexes.[4-11] This state is thought to be mixed quantum-mechanically and not via thermal equilibrium. Thus, spin-orbit coupling provides a mechanism for mixing closely spaced "pure" $S = {}^5/_2$ and ${}^3/_2$ states.

Several porphyrin complexes have been prepared which are thought to show quantum-mechanical spin admixture.[4-11] The structures have been solved for iron(III) tetraphenylporphyrin perchlorate ($Fe(TPP)ClO_4$),[8,9] iron(III) tetraphenylporphyrin tricyanomethanide ($Fe(TPP)C(CN)_3$),[10] and iron(III) octaethylporphyrin perchlorate ($Fe(OEP)ClO_4$).[6] For the tricyanomethanide species a pure $S = {}^3/_2$ configuration has been assigned in the solid state on the basis of Mössbauer quadrupole splitting and structural parameters. Solution studies reported for various perchlorate complexes indicate that spin admixture ($S = {}^5/_2, {}^3/_2$) is not restricted to the solid state.[4] This admixed spin state has been postulated for cytochrome $c'$ on the basis of reduced magnetic moment values and unusual $g = 4$ ESR signals.[12]

Solution properties of weak-field complexes have been examined in detail by multinuclear NMR methods. Rationale for this additional work is found in attempts to unequivocally demonstrate that the anionic ligand remains bound in solution and interest in examining a species with a potentially pure $S = {}^3/_2$ state. It will be demonstrated that perchlorate, trifluoromethanesulfonate, and tricyanomethanide ligands do indeed remain coordinated to synthetic iron(III) porphyrins in nonligating solvents. Further, it is shown that the pure $S$

(1) Scheidt, W. R. In "The Porphyrins"; Dolphin, D., Ed.; Academic Press: New York, 1978; Vol. III, Chapter 10.
(2) La Mar, G. N.; Walker, F. A. In "The Porphyrins"; Dolphin, D., Ed.; Academic Press: New York, 1978; Vol. IV, Chapter 2.
(3) (a) Mashiko, T.; Kastner, M. E.; Spartalian, K.; Scheidt, W. R.; Reed, C. A. *J. Am. Chem. Soc.* **1978**, *100*, 6354. (b) Scheidt, W. R.; Cohen, I. A.; Kastner, M. E. *Biochemistry* **1979**, *18*, 3546.
(4) Goff, H.; Shimomura, E. *J. Am. Chem. Soc.* **1980**, *102*, 31.
(5) Kobayashi, H.; Kaizu, Y.; Eguchi, K. *Adv. Chem. Ser.* **1980**, *No. 191*, 327.
(6) Masuda, H.; Taga, T.; Osaki, K.; Sugimoto, H.; Yoshida, Z.; Ogoshi, H. *Inorg. Chem.* **1980**, *19*, 950.
(7) Ogoshi, H.; Sugimoto, H.; Yoshida, Z. *Biochim. Biophys. Acta* **1980**, *621*, 19.
(8) Reed, C. A.; Mashiko, T.; Bentley, S. P.; Kastner, M. E.; Scheidt, W. R.; Spartalian, K.; Lang, G. *J. Am. Chem. Soc.* **1979**, *101*, 2948.
(9) Kastner, M. E.; Scheidt, W. R.; Mashiko, T.; Reed, C. A. *J. Am. Chem. Soc.* **1978**, *100*, 666.
(10) Summerville, D. A.; Cohen, I. A.; Hatano, K.; Scheidt, W. R. *Inorg. Chem.* **1978**, *17*, 2906.
(11) Dolphin, D. H.; Sams, J. R.; Tsin, T. B. *Inorg. Chem.* **1977**, *16*, 711.
(12) Maltempo, M. M. *J. Chem. Phys.* **1974**, *61*, 2540.

0020-1669/82/1321-0581$01.25/0 © 1982 American Chemical Society

= $^3/_2$ state assigned to Fe(TPP)C(CN)$_3$ in the crystalline form is a consequence of "solid-state" effects, as solution NMR results favor $S = {}^5/_2, {}^3/_2$ admixture.

## Experimental Section

**Solvents.** Hydrocarbon and chlorinated solvents were purified by washing with concentrated $H_2SO_4$ (until the $H_2SO_4$ is colorless), washing twice with water, twice with 10% aqueous $Na_2CO_3$ solution, and twice with water, and drying with a dehydrating agent. The solvents were then distilled into brown bottles containing 3-Å activated molecular sieves. Deuterated chloroform was also distilled into vials containing 3-Å sieves.

**Iron(III) Porphyrin μ-Oxo-Bridged Dimers.** Iron(III) tetraphenylporphyrin (Fe(TPP)X) compounds and the similar Fe(TPP)(R)X compounds (where R is a phenyl ring substituent) were prepared by literature methods.[13-15] The iron(III) octaethylporphyrins (Fe(OEP)X) and iron(III) etioporphyrins (Fe(ETIO)X) were obtained by condensation of the appropriate pyrrole,[16] insertion of the iron to form the chloride monomer, and chromatographic purification.[14] Iron(III) porphyrins were converted to the μ-oxo dimer by shaking a methylene chloride solution with 1 M aqueous NaOH and passing the iron porphyrin solution through a basic alumina column. Microcrystalline products were generally obtained by slow evaporation of methylene chloride with addition of heptane. This dimerization and the following porphyrin reactions were monitored by visible–UV spectra, and final products were characterized by NMR. All iron porphyrin final products were dried several hours at 100 °C under high vacuum.

**Fe(TPP)$SO_3CF_3$** was prepared by dissolving the μ-oxo dimer in $CH_2Cl_2$ (5 mM) and stirring with 3 M aqueous $HSO_3CF_3$ (Aldrich) for 1 h. The layers were separated, and the porphyrin was crystallized by adding heptane. Anal. Calcd for $C_{45}H_{28}N_4O_3F_3SFe$: C, 66.10; H, 3.45; N, 6.85; F, 6.97; Fe, 6.83. Found: C, 66.23; H, 3.87; N, 6.69; F, 6.93; Fe, 7.01. $\lambda_{max}$ ($CH_2Cl_2$): 671 nm ($\epsilon$ 2.4 × 10$^3$), 583 (2.5 × 10$^3$), 515 (1.2 × 10$^4$), and 399 (1.1 × 10$^5$). $\lambda_{max}$(toluene): 672, 657, 581, 512, 422, and 400 nm.

**Fe(TPP)(pyrr-$d_8$)$SO_3CF_3$** (pyrr = pyrrole) was prepared by a modified literature method used to exchange pyrrole protons.[17] Propionic acid-*d* was made by refluxing briefly equimolar amounts of $D_2O$ and propionic anhydride. Pyrrole was added, and the mixture was brought to reflux for 30 min under a nitrogen atmosphere. Air was introduced into the reaction flask, and an appropriate amount of benzaldehyde was added with standard TPP synthesis conditions being applied.[13] Iron was inserted and the trifluoromethanesulfonate ligand added as described previously. The deuterated complex gave the same visible spectrum as Fe(TPP)$SO_3CF_3$.

**Fe(OEP)$SO_3CF_3$** was prepared by cleavage of the μ-oxo dimer as described above. Anal. Calcd for $C_{37}H_{44}N_4O_3F_3SFe$: C, 60.24; H, 6.01; N, 7.59; F, 7.73; Fe, 7.57. Found: C, 60.17; H, 6.22; N, 7.58; F, 7.83; Fe, 7.55. $\lambda_{max}$($CH_2Cl_2$): 632 (2.9 × 10$^3$), 504 (1.0 × 10$^4$), and 383 (1.4 × 10$^5$).

**Fe(ETIO)$SO_3CF_3$** was prepared as above. $\lambda_{max}$($CH_2Cl_2$): 633 nm (2.5 × 10$^3$), 502 (9.3 × 10$^3$), and 384 (1.3 × 10$^5$).

**Fe(TPP)$CO_2CF_3$** was prepared as above except 1 M $HCO_2CF_3$ (Aldrich) was used instead of the $HSO_3CF_3$. Anal. Calcd for $C_{46}H_{28}N_4O_2F_3Fe$: C, 70.69; H, 3.61; N, 7.17; F, 7.30. Found: C, 70.62; H, 3.66, N, 7.09; F, 6.89. $\lambda_{max}$($CH_2Cl_2$): 682, 652, 576, 508, and 414 nm.

**Fe(TPP)(*p*-$OCH_3$)$ClO_4$** was prepared as described in the literature.[4]

**$KC(CN)_3$.** Malonitrile (10 g) and potassium bromide (7.5 g) were dissolved in water (100 mL), and over a period of time at 5 °C bromine (50 g) was added to the stirred solution.[18] The dibromomalonitrile–potassium bromide complex produced was removed by filtration and washed with water. The product was then dried over $P_2O_5$ under high vacuum for 10 h (25 °C). Potassium cyanide (10 g) was added to dimethoxyethane (85 mL), and after the solution was cooled the potassium bromide complex was added and the mixture was stirred for 1.5 h. The solution was heated to reflux briefly and filtered on a hot medium fritted funnel. After the solution cooled overnight, the potassium tricyanomethanide was crystallized by adding ether and was removed by filtration.[19] The labeled compound $NaC(CN)_2(^{13}CN)$ was prepared by substituting $Na^{13}CN$ in place of KCN.

**$Bu_4NC(CN)_3$** was prepared by mixing solutions of $Bu_4NClO_4$ (6 g) in methanol (100 mL) and $KC(CN)_3$ (2.6 g) in methanol (50 mL). Enough methylene chloride (150 mL) was added to ensure that all the $Bu_4NC(CN)_3$ was in solution and the insoluble $KClO_4$ was removed by filtration. $Bu_4NC(CN)_3$ was obtained as an oil following rotary evaporation of the solvents.

**Fe(TPP)$C(CN)_3$** was synthesized by stirring 0.1 g of the μ-oxo dimer in 100 mL of methylene chloride with 0.3 g of $KC(CN)_3$ in 15 mL of 1 M $H_2SO_4$ (aqueous) for 1 h, and the product was crystallized by adding heptane. Anal. Calcd of $C_{48}H_{28}N_7Fe$: C, 75.99; H, 3.72; N, 12.92; Fe, 7.36. Found: C, 75.55; H, 3.87; N, 12.64; Fe, 7.34. $\lambda_{max}$($CH_2Cl_2$): 686 nm (2.9 × 10$^3$), 574 (6.0 × 10$^3$), 519 (1.4 × 10$^4$), and 402 (1.2 × 10$^5$).

**Fe(TPP)$C(CN)_2(^{13}CN)$** was prepared as above, except the labeled compound, $NaC(CN)_2(^{13}CN)$ was used instead of $KC(CN)_3$.

**Fe(OEP)$C(CN)_3$** was prepared as above. Anal. Calcd of $C_{40}H_{44}N_7Fe$: C, 70.79; H, 6.54; N, 14.45; Fe, 8.23. Found: C, 69.94; H, 6.60; N, 14.21; Fe, 8.26. $\lambda_{max}$($CH_2Cl_2$): 627 nm (3.1 × 10$^3$), 507 (1.2 × 10$^4$), and 383 (1.2 × 10$^5$).

## Physical Measurements

Proton NMR spectra were recorded on a JEOL FX-90Q Fourier transform instrument irradiating at 89.56 MHz and using 12–14-kHz sweep widths. The carbon-13 spectra were obtained both on this instrument and on a Bruker HX-90E spectrometer, irradiating at 22.6 MHz and using a 40-kHz sweep width. The shorter probe ring-down time of the JEOL FX-90Q instrument facilitated detection of broad carbon-13 signals, and accordingly this spectrometer was utilized to locate very broad features. Fluorine-19 and chlorine-35 NMR measurements were performed on the multinuclear JEOL FX-90Q spectrometer.

Carbon–hydrogen–nitrogen analysis was performed both at the University of Iowa on a Perkin-Elmer Model 240 Elemental Analyzer and at Galbraith Laboratories, Knoxville, TN. Fluorine analysis was carried out at Galbraith Laboratories. Iron analysis was performed by a spectrophotometric *o*-phenanthroline method following thorough digestion of iron porphyrins by nitric and sulfuric acids.[20,21]

The Evans NMR method was used to obtain values for $\mu_{eff}$.[22,23] Measurements were carried out with 20 mM porphyrin in $CDCl_3$ with 1% $Me_4Si$ used as an internal reference. Changes in densities (and therefore the concentration) were taken into account at the various temperatures.[24-26]

Visible–UV spectra were measured with a Beckman Model 25 spectrophotometer using methylene chloride as the solvent and reference in 1.0-cm quartz cells.

Cyclic voltametry was performed with methylene chloride solvent, and the reference electrode used was Ag/0.01 M $AgNO_3$/acetonitrile. Potentials are reported with respect to the SCE with use of an experimentally determined conversion factor of 0.33 V. The working and counterelectrodes were a platinum bead and coil, respectively. Measurements were made with a Princeton Applied Research (PAR) Model 173 Potentiostat driven by the Model 175 Universal Programmer, using 50 mV/s scan rates.

Electron spin resonance spectra were obtained on a Varian Model V-4502 X-band spectrometer. Samples were run in chloroform at 77 K.

## Results

**Proton NMR Spectroscopy.** Unpaired spin in the $d_{x^2-y^2}$ orbital is associated with predominant σ-spin delocalization

(13) Adler, A. D.; Longo, F. R.; Finarelli, J. D.; Goldmacher, J.; Assour, J.; Korsakoff, L. *J. Org. Chem.* **1967**, *32*, 476.
(14) Adler, A. D.; Longo, F. R.; Vardi, V. *Inorg. Synth.* **1976**, *16*, 213.
(15) Adler, A. D.; Longo, F. R.; Kampus, F.; Kim, J. *J. Inorg. Nucl. Chem.* **1970**, *32*, 2443.
(16) Fuhrhop, J.-H.; Smith, K. M. In "Porphyrins and Metalloporphyrins"; Smith, K. M., Ed.; Elsevier: Amsterdam, 1975; pp 765–770.
(17) Fajer, J.; Borg, D. C.; Forman, A.; Felton, R. H.; Vegh, L.; Dolphin, D. *Ann. N.Y. Acad. Sci.* **1973**, *206*, 349.
(18) Carboni, R. A. *Org. Synth.* **1959**, *39*, 64.
(19) Trofimenko, S.; Little, E. J.; Mower, H. F. *J. Org. Chem.* **1962**, *27*, 433.
(20) Phillippi, M. A. Ph.D. Dissertation, University of Iowa, 1980.
(21) Willard, H. H.; Merritt, L. L.; Dean, J. A. "Instrumental Methods of Analysis", 5th ed.; D. Van Nostrand: Princeton, NJ, 1974.
(22) Evans, D. F. *J. Chem. Soc.* **1959**, 2003.
(23) Eaton, S. S.; Eaton, G. R. *Inorg. Chem.* **1980**, *19*, 1096.
(24) Ostfeld, D.; Cohen, I. A. *J. Chem. Educ.* **1972**, *49*, 829.
(25) Washburn, E. W. "International Critical Tables of Numerical Data"; McGraw-Hill: New York, 1928; Vol. 37, p 27.
(26) "CRC Handbook of Chemistry and Physics"; Weast, R. C., Ed.; Chemical Rubber Co.: Cleveland, OH, 1975; p E128.

Table I. Proton NMR Spectra of Spin-Admixed Complexes[a]

| complex (solvent) | para phenyl | ortho phenyl | meta phenyl | pyrrole |
|---|---|---|---|---|
| $Fe(TPP)SO_3CF_3$ ($CDCl_3$) | 7.49 | *b* | 12.5 | 39.3 |
| $Fe(TPP)C(CN)_3$ ($CDCl_3$) | 7.59 | 9.1 | 12.5 | 24.0 |
| $Fe(TPP)CO_2CF_3$ ($CDCl_3$) | 6.87 | 8.1 | 11.9/12.9 | 74.0 |
| $Fe(TPP)SO_3CF_3$ (toluene) | *d* | 10.1[e] | 12.0/12.8 | 50.4 |
| $Fe(TPP)C(CN)_3$ (toluene) | 7.46 | 11.4[e] | 12.1 | 28.2 |
| $Fe(TPP)ClO_4$[c] ($CDCl_3$) | 7.70 | 9.2 | 11.9 | 13.0 |

| complex (solvent) | meso | methyl | methylene |
|---|---|---|---|
| $Fe(OEP)SO_3CF_3$ ($CDCl_3$) | −24.6 | 7.2[d] | 34.6/49.4 |
| $Fe(OEP)C(CN)_3$ ($CDCl_3$) | −20.2 | 7.46 | 40.5/51.2 |
| $Fe(OEP)ClO_4$[c] ($CDCl_3$) | −5.5 | 6.38 | 35.5 |

| complex (solvent) | meso | methyl (ethyl) | methylene | methyl (ring) |
|---|---|---|---|---|
| $Fe(ETIO)SO_3CF_3$ ($CDCl_3$) | −23.4 | *d* | 34.5/49.2 | 63.8 |
| $Fe(ETIO)ClO_4$[c] ($CDCl_3$) | −10.8 | 6.65 | 28.3/43.6 | 64.3 |

[a] 29 °C, 0.01 M, shifts in ppm relative to internal $Me_4Si$. [b] Signal under other phenyl resonances. [c] Reference 4. [d] Signal under solvent resonance. [e] Signal very broad and possibly split with part of the doublet under other phenyl resonances.

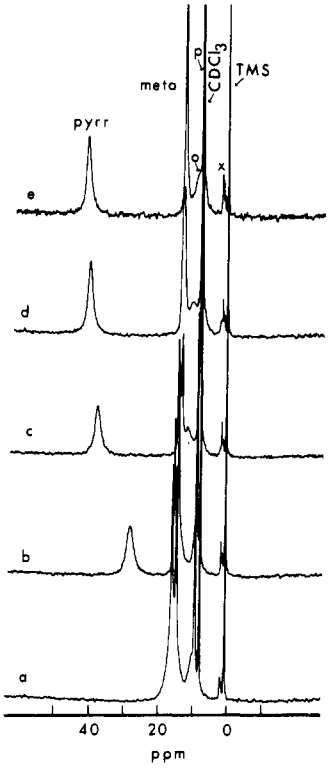


**Figure 1.** Proton NMR spectra of $Fe(TPP)SO_3CF_3$, 0.01 M in $CDCl_3$ (referenced to $Me_4Si$): (a) −58 °C; (b) −40 °C; (c) 0 °C; (d) 29 °C; (e) 55 °C.

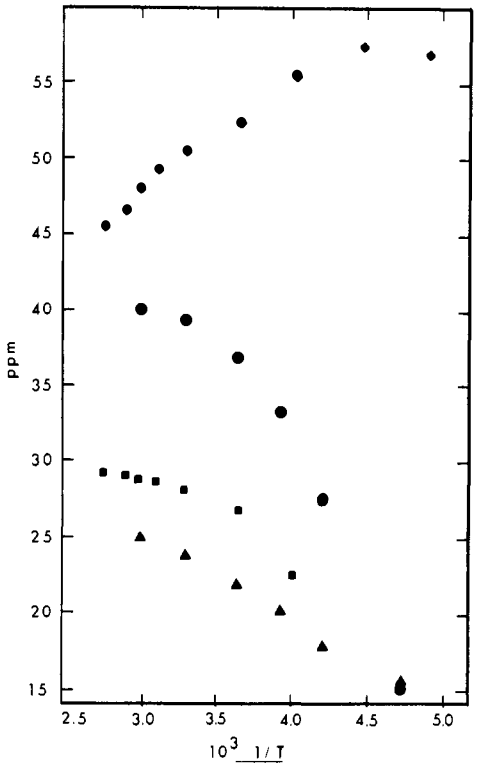


**Figure 2.** Curie law plots of pyrrole proton resonances (iron porphyrin 0.01 M, chemical shifts referenced to $Me_4Si$): ●, $Fe(TPP)SO_3CF_3$ in $CDCl_3$; ▲, $Fe(TPP)C(CN)_3$ in $CDCl_3$; ■, $Fe(TPP)C(CN)_3$ in toluene-$d_8$; ♦, $Fe(TPP)SO_3CF_3$ in toluene-$d_8$.

and downfield pyrrole proton isotropic shifts. Unpaired spin in $d_{xz}$ and $d_{yz}$ orbitals on the other hand makes for upfield pyrrole proton isotropic shifts through a $\pi$-spin delocalization mechanism.[2,4] Proton NMR resonances are thus quite sensitive to the $S = {}^5/_2$ and $S = {}^3/_2$ contributions in a spin-admixed complex. Table I summarizes the proton NMR spectra taken at room temperature in $CDCl_3$ solvent. The peak assignments for $Fe(TPP)SO_3CF_3$ and $Fe(TPP)C(CN)_3$ were made by examining the porphyrins with various substituents on the phenyl positions. The following compounds were used: Fe(TPP)(R)X, where X = $C(CN)_3^-$ or $SO_3CF_3^-$, and R = *p*-$CH_3$, *m*-$CH_3$, 3,4,5-$(OCH_3)_3$, or tetraphenyl-$d_{20}$. Assignments for pyrrole-substituted porphyrins were facilitated by preparation of both the octaethylporphyrin and etioporphyrin complexes.

The pyrrole proton resonances of $Fe(TPP)C(CN)_3$ and $Fe(TPP)SO_3CF_3$ are further upfield than in the usual high-spin species (70–80 ppm)[2] but are further downfield than the pyrrole signal of the $Fe(TPP)ClO_4$ species (12 ppm).[4] The meso proton resonances of $Fe(OEP)C(CN)_3$, $Fe(OEP)SO_3CF_3$, and $Fe(ETIO)SO_3CF_3$ fall between the respective values for high-spin iron(III) complexes (−50 ppm) and those for spin-admixed perchlorate complexes (−5 ppm). This would indicate that the two ligands examined here are weak enough to induce some $S = {}^3/_2$ character, but less so than is the case for the perchlorate species. It should be noted that $Fe(TPP)CO_2CF_3$ is essentially high spin, as the pyrrole proton resonance showed up in the high-spin region (74 ppm).

Variable-temperature measurements are more convincing in terms of demonstrating $S = {}^5/_2, {}^3/_2$ spin admixture. For simple, magnetically ideal paramagnetic molecules, the isotropic shift values are expected to follow Curie law behavior. Thus, the absolute values of the isotropic shift should increase in proportion to $1/T$. This is clearly not the situation for $Fe(TPP)SO_3CF_3$ as is shown in Figure 1. The pyrrole proton

resonances are most sensitive and actually show reversed Curie law behavior in moving upfield as the temperature is lowered. This is illustrated in the form of a Curie law plot in Figure 2. The same shift pattern was also apparent for Fe(TPP)C(CN)$_3$. The Curie law plot for the pyrrole signals of Fe(TPP)$CO_2CF_3$ was well-behaved and indicated the iron(III) was in the high-spin state. Tabulation of variable-temperature measurements is available in supplementary tables.

Proton NMR spectra were also taken at various temperatures with toluene as the solvent. There is a definite solvent dependence as the Curie law plot shows in Figure 2. The Fe(TPP)$SO_3CF_3$ species shows a large increase in high-spin character in this solvent and appears to be predominantly high spin, on the basis of the pyrrole proton resonance value and Curie law plot. The solvent dependence is less dramatic for Fe(TPP)C(CN)$_3$.

Titrating the corresponding tetrabutylammonium salts ($Bu_4NSO_3CF_3$ into Fe(TPP)$SO_3CF_3$ and $Bu_4NC(CN)_3$ into Fe(TPP)C(CN)$_3$) induced some line-width changes but little change in chemical shift values. This experiment serves to demonstrate that anomalous isotropic shift values for these complexes do not result from chemical equilibrium involving loss of coordinated ligand.

**Magnetic Measurements.** Solution magnetic measurements ($CDCl_3$ solvent) were made at temperatures ranging from −50 to 60 °C. For Fe(TPP)$SO_3CF_3$, $\mu_{eff}$ values ranged from 5.3 to 5.6 (±0.1) $\mu_B$, respectively. The room-temperature value of 5.6 $\mu_B$ differs slightly from the previously reported solid-state value of 5.4 $\mu_B$.[8] For Fe(TPP)C(CN)$_3$ the low-temperature $\mu_{eff}$ value is 5.4 $\mu_B$, and at high temperature $\mu_{eff}$ = 5.8 $\mu_B$, in reasonable agreement with the solid-state ambient temperature value of 5.4 $\mu_B$.[10] For Fe(OEP)$SO_3CF_3$ values ranged from 5.0 to 5.4 $\mu_B$, and for Fe(OEP)C(CN)$_3$ values ranged from 5.0 to 5.2 $\mu_B$ over the temperature range −50 to 60 °C. These values indicate that the species are not pure high-spin iron(III) complexes, for which $\mu_{eff}$ = 5.9 $\mu_B$ but also that they show a larger fraction of $S = {}^5/_2$ character and less $S = {}^3/_2$ character than the analogous perchlorate species where $\mu_{eff}$ = 5.2 $\mu_B$ (at room temperature).[8]

**Electron Spin Resonance.** Spectra were recorded at 77 K in frozen $CDCl_3$ solutions approximately 5 mM in iron porphyrin. Minor $g$ = 6 signals were subsequently identified by NMR spectroscopy as being from the high-spin iron(III) chloride adduct—the consequence of persistent trace chloride impurities in chloroform solvent. The following $g$ values were obtained: Fe(TPP)($p$-$OCH_3$)$ClO_4$, $g$ = 4.5, 2.0; Fe(TPP)S-$O_3CF_3$, $g$ = 4.3, 2.0; Fe(TPP)C(CN)$_3$, $g$ = 5.2, 2.0; Fe(OEP)$SO_3CF_3$, $g$ = 4.3, 2.0; Fe(OEP)C(CN)$_3$, $g$ = 4.5, 2.1.

**Cyclic Voltammetry.** Attempts to measure the redox potentials for Fe(TPP)$SO_3CF_3$ and Fe(TPP)C(CN)$_3$ (2 mM in $CH_2Cl_2$) with 0.1 M $Bu_4NClO_4$ for the supporting electrolyte yielded values identical with those for Fe(TPP)$ClO_4$. Suspicion of perchlorate displacement of axial ligand was indeed confirmed by an NMR experiment in which $Bu_4NClO_4$ was titrated into a solution of Fe(TPP)$SO_3CF_3$. Both $SO_3CF_3^-$ and $C(CN)_3^-$ are weak ligands, and competition occurs with the large excess of supporting electrolyte.

The redox potentials for Fe(TPP)$SO_3CF_3$ were measured in 0.1 M $Bu_4NSO_3CF_3$. Oxidation waves at +1.08 and +1.39 V vs. SCE resemble those for a large number of anion complexes of iron(III) porphyrins.[27] Reduction potentials of +0.08 and −1.05 V were recorded. The +0.08-V value is considerably anodic of most high-spin iron(III) porphyrin reductions, and in approaching the +0.14 V value for Fe(TPP)$ClO_4$ it apparently reflects the weak ligand-binding characteristics of $SO_3CF_3^-$.[28]

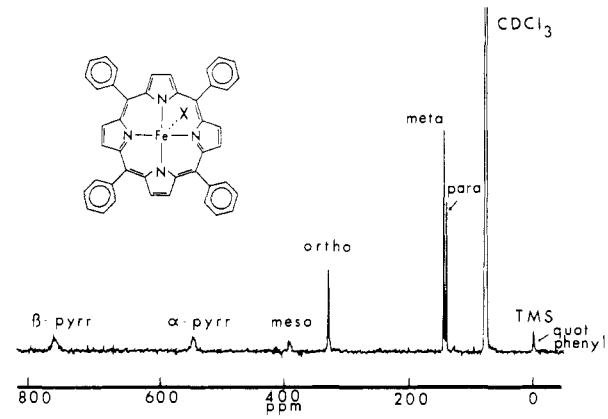


**Figure 3.** Carbon-13 NMR spectrum of Fe(TPP)C(CN)$_3$, 0.05 M in $CDCl_3$, 26 °C, referenced to $Me_4Si$.

**Carbon-13 Spectra.** Carbon-13 NMR spectra gave the same results as the proton spectra in terms of decreased isotropic shift values as compared to those for high-spin iron(III) porphyrins. A typical spectrum of Fe(TPP)C(CN)$_3$ is shown in Figure 3. Variable-temperature experiments also showed non-Curie law behavior. Spectra resemble those for high-spin iron(III) complexes.[29-31] Phenyl resonance assignments were made by using selective frequency decoupling and by comparison with high-spin spectra. The far downfield pyrrole carbon assignments were made possible with the pyrrole deuterated species. A deuterium isotope shift[32] of 6 ppm upfield for Fe(TPP)(pyrr-$d_8$)$SO_3CF_3$ confirmed the $\beta$-pyrrole assignment. The spectrum of a 50:50 mixture of Fe(TPP)S-$O_3CF_3$ and Fe(TPP)(pyrr-$d_8$)$SO_3CF_3$ showed a measurable separation of pyrrole peaks.

Axial ligand carbon signals were not observed at room temperature, even with the labeled ligand in Fe(TPP)C(C-N)$_2$($^{13}$CN). However, the $^{13}$CN signal was seen at −160 ppm (line width 1400 Hz) at −25 °C. The crystal structure indicates the ligand is bound end-on through the nitrogens in the solid state.[10] The ligand signal observed is thought to represent the two uncoordinated nitrile groups, with the coordinated signal broadened beyond detectability. Our inability to observe the signal at room temperature most likely reflects intermolecular exchange of $C(CN)_3^-$ or rotation of $C(CN)_3^-$ with subsequent severe broadening. Other carbon-13 spectra exhibit the same relative shifts as shown in Table II. The spectrum for Fe(ETIO)$SO_3CF_3$ was examined to try to detect splitting of the $\beta$-pyrrole signal as a consequence of attached methyl and methylene groups; however, no splitting was detected.

**Fluorine-19 NMR spectroscopy** was used to examine the binding of $SO_3CF_3^-$ to Fe(TPP)$^+$. The broad, coordinated trifluoromethyl signal for Fe(TPP)$SO_3CF_3$ as shown in Figure 4a is located at −19 ppm (with $CFCl_3$ as an external reference). The fluorine resonance for $Bu_4NSO_3CF_3$ in chloroform is found at −78.7 ppm. When 0.5 equiv of $Bu_4NSO_3CF_3$ was added to the Fe(TPP)$SO_3CF_3$ solution, a very broad signal was observed upfield from that of the Fe(TPP)$SO_3CF_3$ complex (Figure 4b). As the temperature was lowered, this peak split at −55 °C near the slow exchange limit such that individual signals for coordinated and free $SO_3CF_3^-$ are seen (Figure 4c). Addition of more $Bu_4NSO_3CF_3$ at room tem-

(27) Phillippi, M. A.; Shimomura, E. T.; Goff, H. M. *Inorg. Chem.* **1981**, *20*, 1322.

(28) Kadish, K. M.; Bottomley, L. A. *Inorg. Chem.* **1980**, *19*, 832.
(29) Phillippi, M. A.; Goff, H. M. *J. Chem. Soc., Chem. Commun.* **1980**, 455.
(30) Mispelter, J.; Momenteau, M.; Lhoste, J.-M. *J. Chem. Soc., Chem. Commun.* **1979**, 808.
(31) Goff, H. *Biochim. Biophys. Acta* **1978**, *542*, 348.
(32) Detailed investigation of deuterium isotope effects in carbon-13 spectra of a variety of paramagnetic metalloporphyrins is in progress.

Table II. Carbon-13 NMR Spectra of Spin-Admixed Complexes[a]

| complex | quat phenyl | para phenyl | meta phenyl | ortho phenyl | meso | α-pyrrole | β-pyrrole |
|---|---|---|---|---|---|---|---|
| $Fe(TPP)SO_3CF_3$ | −16.2 | 140.6 | 146.6 | 366.7 | 418 | 757 | 911 |
| $Fe(TPP)C(CN)_3$ | 0[b] | 140.6 | 144.6 | 330.6 | 396 | 544 | 778 |

| complex | $CH_2$ | $CH_3$ (ethyl) | $CH_3$ (ring) | meso | α-pyrrole | β-pyrrole |
|---|---|---|---|---|---|---|
| $Fe(OEP)SO_3CF_3$ | 4.0 | 208 | | 300 | 635 | 796 |
| $Fe(ETIO)SO_3CF_3$ | 10.4 | 187 | −2.0 | 286 | 647 | 792 |

[a] Shifts in ppm referenced to $Me_4Si$ (internal), in $CDCl_3$, 0.05 M, 26 °C. [b] Signal under $Me_4Si$.

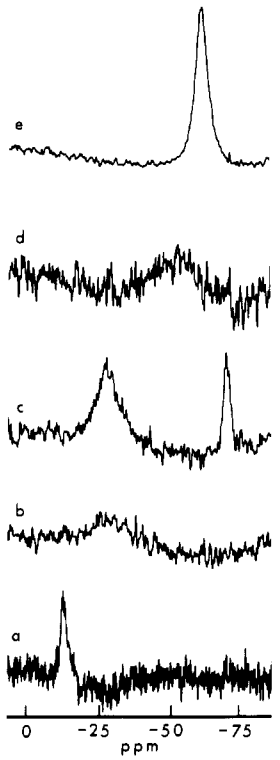


**Figure 4.** Fluorine-19 NMR spectra of titration of $Fe(TPP)SO_3CF_3$ (0.01 M in $CDCl_3$, referenced to external $CFCl_3$): (a) $Fe(TPP)SO_3CF_3$, 29 °C; (b) 0.5 equiv of $Bu_4NSO_3CF_3$ added, 29 °C; (c) 0.5 equiv of $Bu_4NSO_3CF_3$ added, −55 °C; (d) 1.5 equiv of $Bu_4NSO_3CF_3$ added, 29 °C; (e) 5.5 equiv of $Bu_4NSO_3CF_3$ added, 29 °C.

perature yields a mole-fraction-weighted signal approaching that of free $SO_3CF_3^-$ (Figures 4d and 4e).

**Chlorine-35 NMR Spectroscopy.** Attempts were made to locate the chlorine-35 NMR signal in the $Fe(TPP)(p\text{-}OCH_3)ClO_4$ complex with a 40-kHz spectral window and an 8.72-MHz irradiation frequency. No signal was observed, perhaps due to a combination of paramagnetic and quadrupolar line broadening. Sequential addition of 0.5, 1.0, and 2.0 equiv of $Bu_4NClO_4$ did, however, yield signals at 29 °C shifted 106, 58, and 47 ppm downfield from the resonance for a solution containing only $Bu_4NClO_4$. At 50 °C with 1.0 and 2.0 equiv, signals are shifted 160 and 97 ppm downfield. With the assumptions that at 50 °C the fast exchange limit has been reached and that a mole-fraction-weighted average perchlorate signal results, a downfield shift of at least 300 ppm is expected for coordinated perchlorate ion. It should be noted that these experiments were performed with $CDCl_3$ as a solvent but that solvent signal interference presented no problem as quadrupolar relaxation gives extremely broad signals for molecules of noncubic symmetry.

## Discussion

A major objective of this multinuclear NMR study was to distinguish coordination vs. possible tight ion pairing for weak-field ligand complexes in solution. Observation of NMR signals for axial ligands serves to rationalize coordination, although it must be shown that the observed isotropic ligand shift could not result entirely from a dipolar shift for an ion pair. The dipolar shift can be estimated with the equation

$$(\Delta H/H)_{dip} = \frac{1}{3N}(\chi_{\parallel} - \chi_{\perp})\left(\frac{3\cos^2\theta - 1}{r^3}\right)$$

where $r$ is the distance of the observed nucleus from the paramagnetic center and $\theta$ is the angle with respect to the $z$ axis for the metal–nuclear vector.[33] This dipolar term and the contact term make up the total isotropic shift, and relate the through-space and through-bond electron-nuclear interactions, respectively. A general downfield bias of isotropic shift values for phenyl protons of $Fe(TPP)ClO_4$ presumably results predominantly from dipolar shifts, and a downfield dipolar shift of 5.3 ppm was estimated for the ortho phenyl proton.[4] Although the perchlorate complex contains less $S = {}^5/_2$ character than the other species, this value was assumed to provide an approximate (or perhaps inflated) value for the dipolar shift of the ortho phenyl proton in the $SO_3CF_3^-$ and $C(CN)_3^-$ adducts. So that an upper limit could be placed on the possible dipolar shifts for an ion-paired ligand, it was assumed that the ligand nuclei of interest were located on or near the $z$ axis ($\theta = 0°$). Note that this maximizes the dipolar shift and reverses the sign with respect to the ortho phenyl proton value. Two of the nitrile carbons in the tricyanomethanide ligand were assumed to be in positions similar to the unbound nitrile groups in the crystal structure ($r = 5.3$ Å, $\theta = 15°$), and the bound position was used for the third carbon ($r = 3.5$ Å).[10] Values were taken from the crystal structure for $Fe(TPP)ClO_4$ distances ($r = 3.5$ Å).[8] An appproximate value of $r$ (6.6 Å) for the fluorine atoms of trifluoromethanesulfonate ligand was obtained from general bond lengths[34] and the iron–oxygen bond length from the perchlorate structure.[8]

The peak for chlorine-35 in $Fe(TPP)(p\text{-}OCH_3)ClO_4$ is shifted at least 300 ppm downfield. This value is considerably different in both magnitude and direction than the maximum upfield dipolar shift value of −75 ppm. Likewise, the fluorine-19 signal in $Fe(TPP)SO_3CF_3$ is 60 ppm downfield ($Bu_4NSO_3CF_3$) as compared with the maximum calculated dipolar value of −11 ppm. The maximum dipolar shift of the nitrile carbon in the tricyanomethanide ligand is calculated to be −39 ppm, but the observed signal is located at −160 ppm (−25 °C). In conclusion, the large isotropic shifts observed for nuclei of the three anions cannot be explained by maximal dipolar shifts possible for a strong ion paired structure. Contact shifts in a coordinated structure must be invoked.

It has been observed that the first iron(III) porphyrin reduction wave qualitatively indicates the bonding strength of the axial ligand for the halides[35,36] and seems to hold for other ligands as well. The reduction potential for $Fe(TPP)SO_3CF_3$

(33) Horrocks, W. DeW. In "NMR of Paramagnetic Molecules"; La Mar, G. N., Horrocks, W. DeW., Holm, R. H., Eds.; Academic Press: New York, 1973; pp 127–177.
(34) "CRC Handbook of Chemistry and Physics"; Weast, R. C., Ed.; Chemical Rubber Co.: Cleveland, OH, 1975; pp F211–F213.
(35) Lexa, D.; Momenteau, M.; Mispelter, J.; Lhoste, J. M. *Bioelectrochem. Bioenerg.* **1974**, *1*, 108.
(36) Boucher, L. J.; Garber, H. K. *Inorg. Chem.* **1970**, *9*, 2644.

($E_{1/2}$ = 0.08) is more negative than the value for $Fe(TPP)ClO_4$ ($E_{1/2}$ = 0.14) but less negative than that of the usual chloride high-spin derivative ($E_{1/2}$ = −0.29), indicating the bonding strength is greater for $Fe(TPP)SO_3CF_3$ than for $Fe(TPP)ClO_4$ but weaker than for the high-spin complexes. This evidence is complemented by the order of pyrrole proton resonances of $Fe(TPP)SO_3CF_3$ > $Fe(TPP)C(CN)_3$ > $Fe(TPP)ClO_4$. Also, the Soret band and the ~500-nm region band positions follow an order parallel to the NMR and cyclic voltametry results. With toluene as the solvent, the Soret bands for Fe(TPP)Cl, $Fe(TPP)SO_3CF_3$, and $Fe(TPP)ClO_4$ are located at 402, 408, and 415 nm, respectively. In contrast, the major visible region band is increased in energy from 518 to 512 to 505 nm for Fe(TPP)Cl, $Fe(TPP)SO_3CF_3$, and $Fe(TPP)ClO_4$, respectively. The other absorption bands are not as well defined. This indicates that the trifluoromethanesulfonate ligand is bound more strongly than the perchlorate ion but weaker than in the high-spin halide compounds. Thus, the order of ligand strengths appears to be halide ≫ $SO_3CF_3^-$ > $C(CN)_3^-$ > $ClO_4^-$. The ESR $g_\perp$ values, however, do not follow a clear pattern in that $g_\perp$ = 5.2 for $Fe(TPP)C(CN)_3$, but the $g_\perp$ value for $Fe(TPP)SO_3CF_3$ (4.3) is lower than that for $Fe(TPP)(p\text{-}OCH_3)ClO_4$ (4.5).[8] Variable zero-field-splitting values among the anionic complexes could serve to explain the lack of correspondence.

An unusual solid-state structure is found for the $C(CN)_3^-$ complex, in which the anion serves as a bridging ligand to make the iron center six-coordinate. Structural and Mössbauer parameters have been interpreted to favor a pure $S = {}^3/_2$ state in the solid.[10] In solution the complex appears to be five-coordinate, as judged by splitting of the meta phenyl proton signal at low temperature. A pure $S = {}^3/_2$ complex is expected to have the pyrrole proton resonance shifted in a far upfield position through a $\pi$-type unpaired spin delocalization mechanism.[4] However, the observed downfield position and anomalous temperature dependence is consistent with $S = {}^5/_2$, ${}^3/_2$ spin admixture. The possible appearance of a pure $S = {}^3/_2$ configuration for the $C(CN)_3^-$ complex may thus be described as a "solid-state effect".

**Acknowledgment.** Support from NSF Grant CHE 79-10305 is gratefully acknowledged.

**Registry No.** $Fe(TPP)SO_3CF_3$, 70936-35-5; $Fe(TPP)C(CN)_3$, 25704-06-7; $Fe(TPP)CO_2CF_3$, 79872-93-8; $Fe(OEP)SO_3CF_3$, 79872-94-9; $Fe(OEP)C(CN)_3$, 80105-66-4; $Fe(ETIO)SO_3CF_3$, 79898-45-6.

**Supplementary Material Available:** Tables of proton and carbon-13 NMR shift values (6 pages). Ordering information is given on any current masthead page.

---

Contribution from the Department of Physical and Inorganic Chemistry, The University of New England, Armidale, NSW, Australia, 2351

# Exchange Interactions in the Linear-Chain Compounds Azidobis(pentane-2,4-dionato)manganese(III) and (Thiocyanato)bis(pentane-2,4-dionato)manganese(III)

ANTHONY K. GREGSON* and NEVILLE T. MOXON

*Received November 20, 1980*

Powder magnetic measurements on the linear-chain compounds $Mn(acac)_2X$ (Hacac = pentane-2,4-dione; X = $N_3^-$, $NCS^-$) show the presence of antiferromagnetic intrachain interaction. The one-dimensional Heisenberg model leads to $J(N_3)$ = 5.3 $cm^{-1}$ and $J(NCS)$ = 1.5 $cm^{-1}$. Sharp increases in the susceptibilities precede phase transitions at 11.3 and 6.9 K, respectively, and are probably the result of a small canting introduced by the zero-field splitting associated with the Mn(III) ion.

## Introduction

Octahedral complexes of high-spin Mn(III) are interesting because they are expected to be susceptible to Jahn–Teller distortions causing them to deviate from idealized $O_h$ symmetry, either by a trigonal distortion or by a tetragonal compression or elongation. This is well illustrated by the recent structural work on the $\beta^1$ and $\gamma^2$ forms of $Mn(acac)_3$ (Hacac = pentane-2,4-dione) and $Mn(trop)_3$[3] (Htrop = tropolone). The magnetic properties of $\beta$-$Mn(acac)_3$ and $Mn(trop)_3$ have also been shown to be compatible with the different types of distortion found in these structures.[4]

A new series of high-spin Mn(III) complexes having the general formula $Mn(acac)_2X$ (X = $N_3^-$, $NCS^-$) has been prepared and characterized recently.[5] The crystal structures of both materials[5,6] showed that, rather than being 5-coordinate, the Mn(III) ion was 6-coordinate, the anionic $N_3$ or NCS bridge adjacent metal ions forming a chain (Figure 1). In both cases a tetragonally elongated octahedral coordination polyhedron about the Mn(III) ion was present. We have been interested in the magnetic properties of metal $\beta$-diketonate compounds[4,7,8] particularly when the structures indicate the possibility of exchange interaction.[4,8] In the present case we might anticipate magnetic interaction to be associated with the polymeric one-dimensional chains. Accordingly we report here the low-temperature magnetic properties of $Mn(acac)_2N_3$ and $Mn(acac)_2NCS$ where we show that there is significant intrachain-exchange interaction present.

## Experimental Section

The two compounds were prepared by previously published methods.[5,6] $MnSO_4 \cdot 4H_2O$ was dissolved in water, Hacac and $KMnO_4$ were added, and the solution was stirred for 15 min. KSCN was then added with stirring for a further 30 min. The olive green precipitate

(1) Fackler, J. P.; Avdeef, A. *Inorg. Chem.* **1974**, *13*, 1864.
(2) Stults, B. R.; Marianelli, R. S.; Day, V. W. *Inorg. Chem.* **1979**, *18*, 1853.
(3) Avdeef, A.; Costamagna, A.; Fackler, J. P. *Inorg. Chem.* **1974**, *13*, 1854.
(4) Gregson, A. K.; Doddrell, D. M.; Healy, P. C. *Inorg. Chem.* **1978**, *17*, 1216.
(5) Stults, B. R.; Marianelli, R. S.; Day, V. W. *Inorg. Chem.* **1975**, *14*, 722.
(6) Stults, B. R.; Day, R. O.; Marianelli, R. S.; Day, V. W. *Inorg. Chem.* **1979**, *18*, 1847.
(7) Moxon, N. T.; Gregson, A. K. *J. Inorg. Nucl. Chem.* **1981**, *43*, 491.
(8) Gregson, A. K.; Anker, M. *Aust. J. Chem.* **1979**, *32*, 503.

0020-1669/82/1321-0586$01.25/0 © 1982 American Chemical Society